Supporting Information: Selective gas capture via kinetic trapping

Joyjit Kundu,* Tod Pascal, David Prendergast and Stephen Whitelam‡

S1 Simulation details

Eq. (1) of the main text follows from the condition of detailed balance applied to our Monte Carlo protocol. In general, we consider gas mixtures of variable composition, and specialize in the main text to the case of an equimolar mixture. The sum of rates of all microscopic process is $R \equiv L_y R_\mathrm{i} + n_0 R_\mathrm{r} + n R_\mathrm{d}$, where L_y is the number of sites in the left-most column $z = 0$ of the lattice, n_0 is the instantaneous number of particles on the left-most column, and n is the instantaneous total number of particles on the lattice. To enforce detailed balance we consider the interconversion of microstates A and B. Detailed balance requires

$$p(\mathrm{A})\ p_\mathrm{gen}(\mathrm{A}\to\mathrm{B})\ p_\mathrm{acc}(\mathrm{A}\to\mathrm{B}) = p(\mathrm{B})\ p_\mathrm{gen}(\mathrm{B}\to\mathrm{A})\ p_\mathrm{acc}(\mathrm{B}\to\mathrm{A}). \tag{S1}$$

Here $p(i) \propto \exp(-\beta U_i)\prod_j z_j^{n_j}$ is the equilibrium probability of being in microstate i with energy U_i, where n_j is the number of particles of gas type $j \in \{\mathrm{H_2}, \mathrm{CO_2}, \mathrm{H_2O}\}$ in microstate i, and $z_j = \exp(\mu_j/k_\mathrm{B}T)$ is the fugacity of gas type j. p_gen and p_acc are the probabilities of generating and accepting a proposed move.

We choose to attempt diffusion moves with probability nR_d/R. We then choose a particle uniformly from all n particles in the system, and propose to move it to one of its four nearest-neighbor sites. The probability of generating a diffusion move is then $p_\mathrm{gen} = R_\mathrm{d}/(4R)$. From (S1) we can solve for the acceptance rate for a diffusion move,

$$p_\mathrm{acc} = \min\left(1, \frac{R_\mathrm{before}}{R_\mathrm{after}} \mathrm{e}^{-\beta\Delta U}\right). \tag{S2}$$

Here ΔU is the energy difference between the final and initial microstates, and R_before and R_after are the values of $R \equiv L_y R_\mathrm{i} + n_0 R_\mathrm{r} + n R_\mathrm{d}$ before and after the proposed move.

For insertion-removal moves we proceed as follows. We attempt an insertion move with probability $L_y R_i/R(\mathrm{A})$, where $R(\mathrm{A})$ is the total rate calculated in microstate A. A specific site is chosen among L_y sites at random from the left-most column with probability $1/L_y$. We then propose to insert a particle of type j with probability $z_j/\sum_m z_m$, where the sum runs over all gas types. Thus the probability of generating the insertion move is $p_\mathrm{gen}(\mathrm{A}\to\mathrm{B}) = R_i\ z_j/(R(\mathrm{A})\ \sum_m z_m)$.

We attempt a removal move with probability $n_0 R_\mathrm{r}/R(\mathrm{B})$, where $R(\mathrm{B})$ is the total rate calculated in microstate B. A specific particle among n_0 particles in the left-most column is chosen with probability $1/n_0$. The probability of generating the removal move is then $p_\mathrm{gen}(\mathrm{B}\to\mathrm{A}) = R_r/R(\mathrm{B})$. Noting that microstate B contains one more particle of type j than microstate A, we have from (S1) that

$$\frac{p_\mathrm{acc}(\mathrm{A}\to\mathrm{B})}{p_\mathrm{acc}(\mathrm{B}\to\mathrm{A})} = \frac{R(\mathrm{A})}{R(\mathrm{B})}\ e^{-\beta\Delta U}\frac{R_\mathrm{r}}{R_\mathrm{i}}\sum_m z_m. \tag{S3}$$

We further set $\sum_m z_m R_\mathrm{r}/R_\mathrm{i} = 1$ so that the acceptance rates for insertion and removal moves have the form given in (S2). In the main text we consider the case of an equimolar gas mixture, for which all fugacities z_j are the same, and thus, we set $3z_j R_i/R_r = 1$.

In this supplement we present simulation reults for non-equimolar gas mixtures. The composition of a post-combustion flue gas depends on the particulars of the power plant. Often it consists of 70-75% N_2, 12-15% CO_2, 5-7% H_2O, and small amounts of SO_2, NO_x, O_2, CO, etc. H_2 is an important constituent of pre-combustion flue gas, and for Mg-MOF-74 occupies the same position as N_2 in the hierarchy of binding enthalpies and diffusion barriers with respect to CO_2 and H_2O. Fig. S1(a) and (b) present the density of CO_2 as a function of time and temperature for an equimolar gas mixture, while in Fig. S1(c) we show a time-temperature plot for the density of CO_2 when the model framework is exposed to a gas mixture with composition 75% H_2, 15% CO_2 and 10% H_2O. For these simulations z_{H_2}:z_{CO_2}:z_{H_2O}=75:15:10. Our qualitative conclusions are as for the equimolar case: CO_2 can be captured, in abundance, under nonequilibrium conditions.

S2 Estimate of the basic time scale Δt of the model

We determined the basic timescale of our model by comparison with experiment as follows. We set up a simulation to mimic an experiment in which H_2O is passed through Mg-MOF-74 preloaded with bound CO_2 [1]. We measured the time taken by H_2O to displace

*Molecular Foundry, Lawrence Berkeley National Laboratory, Berkeley, CA 94720, USA; * E-mail: jkundu@lbl.gov, ‡ E-mail: swhitelam@lbl.gov*

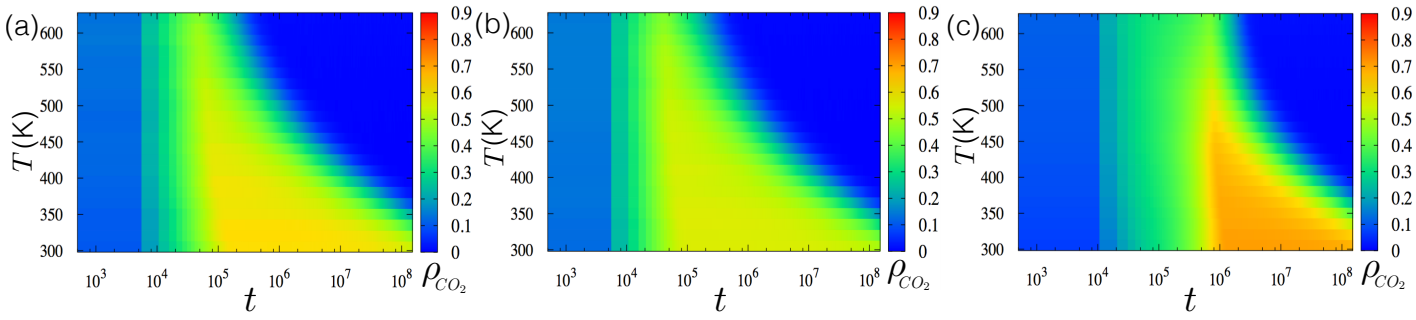

Fig. S1 Bound CO_2 fraction as a function of time t (in units of Δt), for simulations run at a range of temperature T. In panel (a), the values of intra-species pairwise nearest-neighbor repulsive interactions are 0.0025 eV, 0.02 eV, or 0.03 eV for H_2, CO_2 or H_2O, respectively [3]. Inter-species interactions are chosen to be the arithmetic mean of the corresponding intra-species interactions. In panel (b), inter-species interactions are set to zero. In both the cases the framework was in contact with a reservoir of an equimolar gas mixture. In panel (c), the reservoir contains a mixture of 75% H_2, 15% CO_2 and 10% H_2O. Here, the inter-species interactions are the same as those used in panel (a). The data are for $L_y = 40$ and $L_z = 80$.

CO_2. We started the simulation with all binding sites of the framework occupied by CO_2, and then exposed the framework to H_2O. As time progresses, H_2O displaces CO_2, as shown in Fig. S2(a). We define the equilibration time as the time when the bound fraction of H_2O is 99%. Fig. S2(b) shows the equilibration time τ_{eq} as a function of L_z at different temperatures. These data can be fit by the equation

$$\tau_{eq}(T) = \mathrm{A}(T) + \mathrm{B}(T)\, L_z^{\nu(T)}. \tag{S4}$$

We summarize the values of A, B and ν at different temperatures, obtained by fitting the simulation data with Eq. S4, in table 1. We find that $\nu \approx 2$. In the experiment with a sample of thickness 40 μm, H_2O adsorption was found to reach equilibrium after ~ 210 s at

T (K)	A	B	ν
523	1.26×10^6	8.87	2.05
493	2.53×10^6	15.49	1.97
463	5.57×10^6	17.94	1.96
433	1.46×10^7	10.02	2.05
403	4.41×10^7	2.21	2.26
348	5.15×10^8		

Table 1 Values of A, B and ν at different temperatures, measured by fitting the simulation data with Eq. S4.

348 K [1]. Such lengthscales and timescales are out of reach of our simulations, but by extrapolation we can compare those experiments with our results. At 348 K we can estimate the value of $\mathrm{A}(\approx 5.15 \times 10^8)$ by extrapolation: see inset of Fig. S2(a). Using Eq. (S4) and all combinations of B and ν for the different temperatures listed in table 1, we find that the choice $\Delta t \sim 10^{-10}$ s gives the range $\tau_{eq}(348\ \mathrm{K}) \approx 76 - 405$ s, which encompasses the experimental value of 210 s. The value of Δt is physically reasonable: it is close to the measured self-diffusion time of CO_2 in Mg-MOF-74, which is $\sim 10^{-10}$–10^{-9} s [2]. By comparison, the the self-diffusion time of CO_2 in air is $\sim 10^{-16}$–10^{-15} s.

S3 Polydispersity of grain size and nonequilibrium gas capture

In Fig. S4(a) and Fig. S5, we show that nonequilibrium gas capture can be effected in a MOF powder whose grains possess a distribution of sizes. Fig. S4(a) shows the bound fraction of CO_2 (ρ_{CO_2}) as a function of time for different values of L_z at 328 K. The data for the time $\tau_{0.5}$ at which ρ_{CO_2} decays to a value of 0.5, after attaining its maximum value, are plotted against L_z in Fig. S4(b). These data can be fit, at 328 K, by $\tau_{0.5} = C + D\, L_z^m$, where $C \approx 7.45 \times 10^7$, $D \approx 87.71$ and $m \approx 1.77$. Using this fit we can predict the time window within which CO_2 can be captured by a framework. Our results suggest that at 298 K, a framework of length $L_z = L_c \approx 0.43$ μm, exposed to an equimolar mixture of the three gas types considered here, will harbor CO_2 at more than 40% of its binding sites up to a time of ~ 0.1 s. Here, $C(298\ \mathrm{K}) \approx 1.15 \times 10^9$: see Fig. S4(c), as obtained from simulations at 298 K and the values D, m are considered to be same as those at 328K.

References

1 K. Tan, S. Zuluaga, Q. Gong, Y. Gao, N. Nijem, J. Li, T. Thonhauser, and Y. J. Chabal, Chem. Mater. **27**, 2203 (2015).

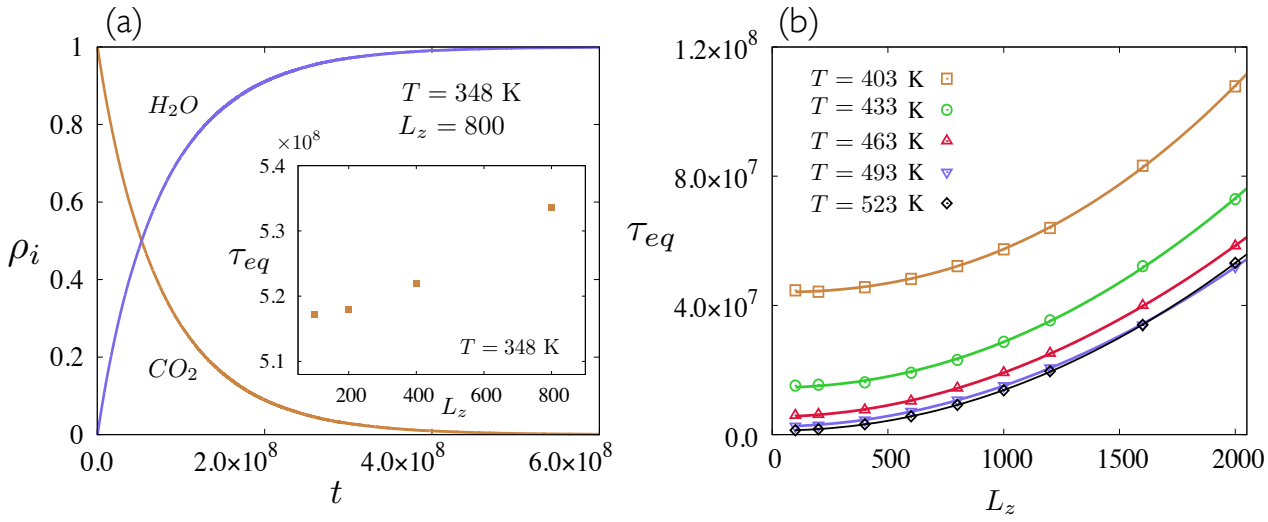

Fig. S2 We fix the basic time scale Δt of our model by comparing the equilibration time in simulation with that measured in an experiment in which a framework pre-loaded with CO_2 is exposed to H_2O[1]. (a) Time evolution of the bound fraction of CO_2 and H_2O at 348 K for $L_z = 800$. Inset: equilibration time τ_{eq} as a function of L_z at 348 K. (b) Equilibration time τ_{eq} as a function of L_z at different temperatures. Data points are obtained from simulations. Solid lines are fits to the data using $\tau_{eq}(T) = A(T) + B(T)\, L_z^{\nu(T)}$. The values of $A(T)$, $B(T)$, and $\nu(T)$ at different temperatures are listed in table 1. The data are averaged over 100 independent simulations and are for $L_y = 10$.

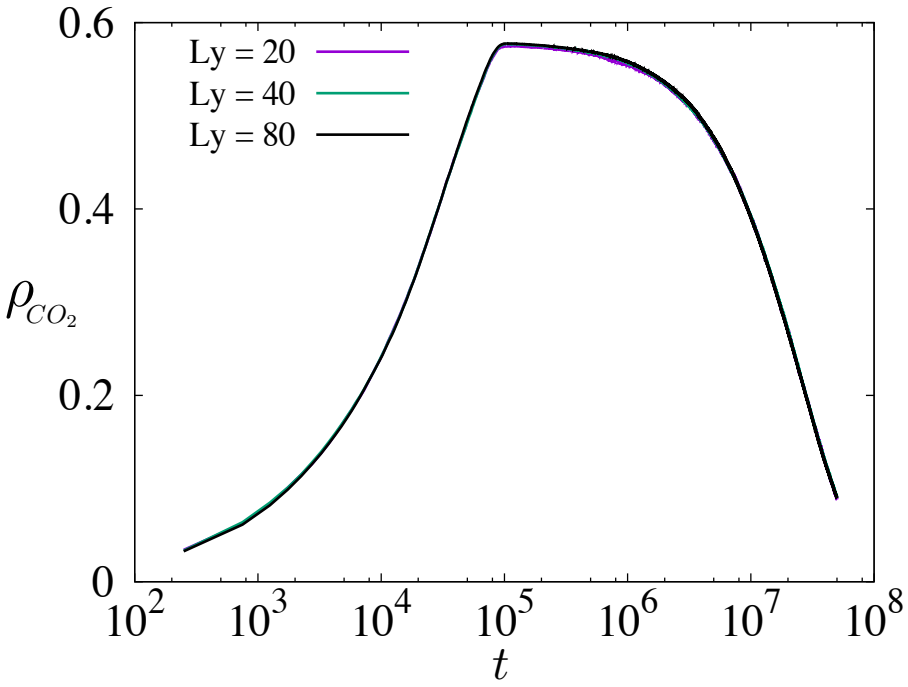

Fig. S3 Simulation results are largely insensitive to the lateral extent L_y of the framework, because motion along channels is effectively one dimensional. We plot ρ_{CO_2} as a function of time t (in units of Δt) for three different values of L_y ($L_z = 80$) at 388 K, averaged over 100 independent runs.

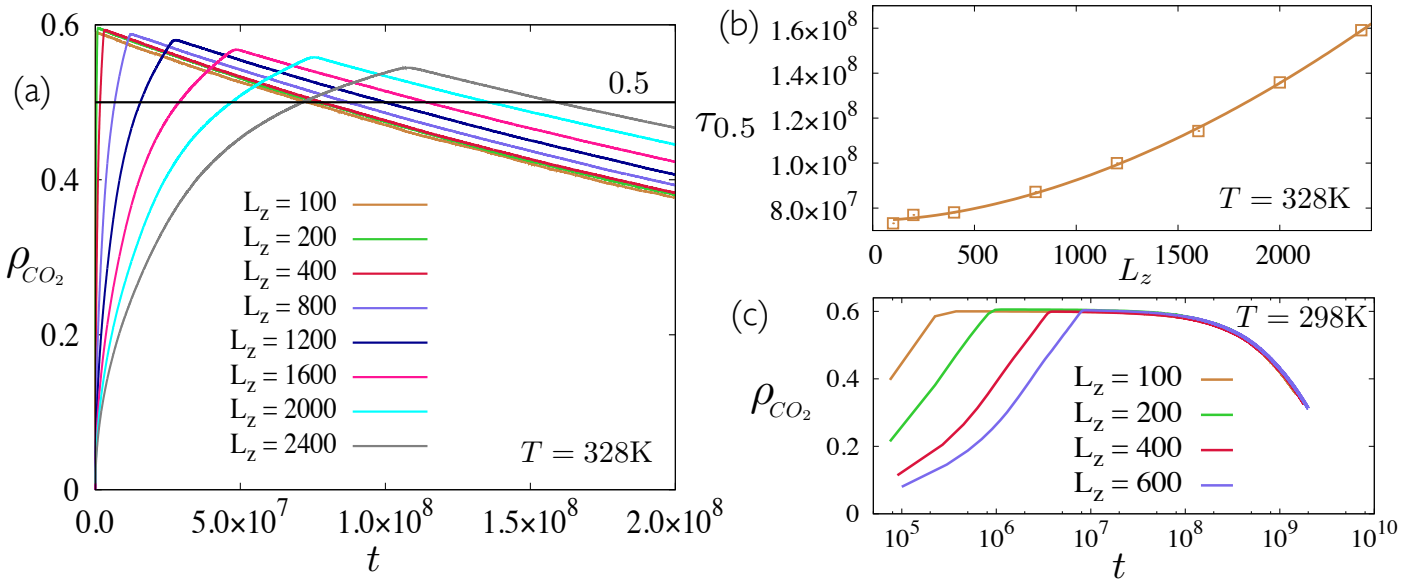

Fig. S4 We can predict the timescale of CO_2 capture, for fixed L_z, under nonequilibrium conditions. (a) Time evolution of ρ_{CO_2}, the bound fraction of CO_2 at 328 K for different L_z. The horizontal line corresponds to $\rho_{CO_2} = 0.5$. (b) The time at which ρ_{CO_2} decays to 0.5 as a function of the linear extent of the framework along z at 328 K. The data points are obtained from simulations; the solid line is a fit to the data and follows the equation $\tau_{0.5} = C + D\,L_z^m$, where $C \approx 7.45 \times 10^7$, $D \approx 87.71$ and $m \approx 1.77$. (c) Time evolution of ρ_{CO_2} at 298 K for four different system sizes. We find $C(298\text{ K}) \approx 1.15 \times 10^9$ by extrapolation. Being unable to go up to larger system sizes, we consider that the value of D and m at 298 K are same as those for 328 K. The data are averaged over 80 independent simulations and are for $L_y = 10$.

2 Z. Bao, L. Yu, Q. Ren, X. Lu, and S. Deng, J. Colloid Interface Sci. **353**, 549 (2011).

3 P. Canepa, N. Nijem, Y. J. Chabal, and T. Thonhauser, Phys. Rev. Lett. **110**, 026102 (2013).

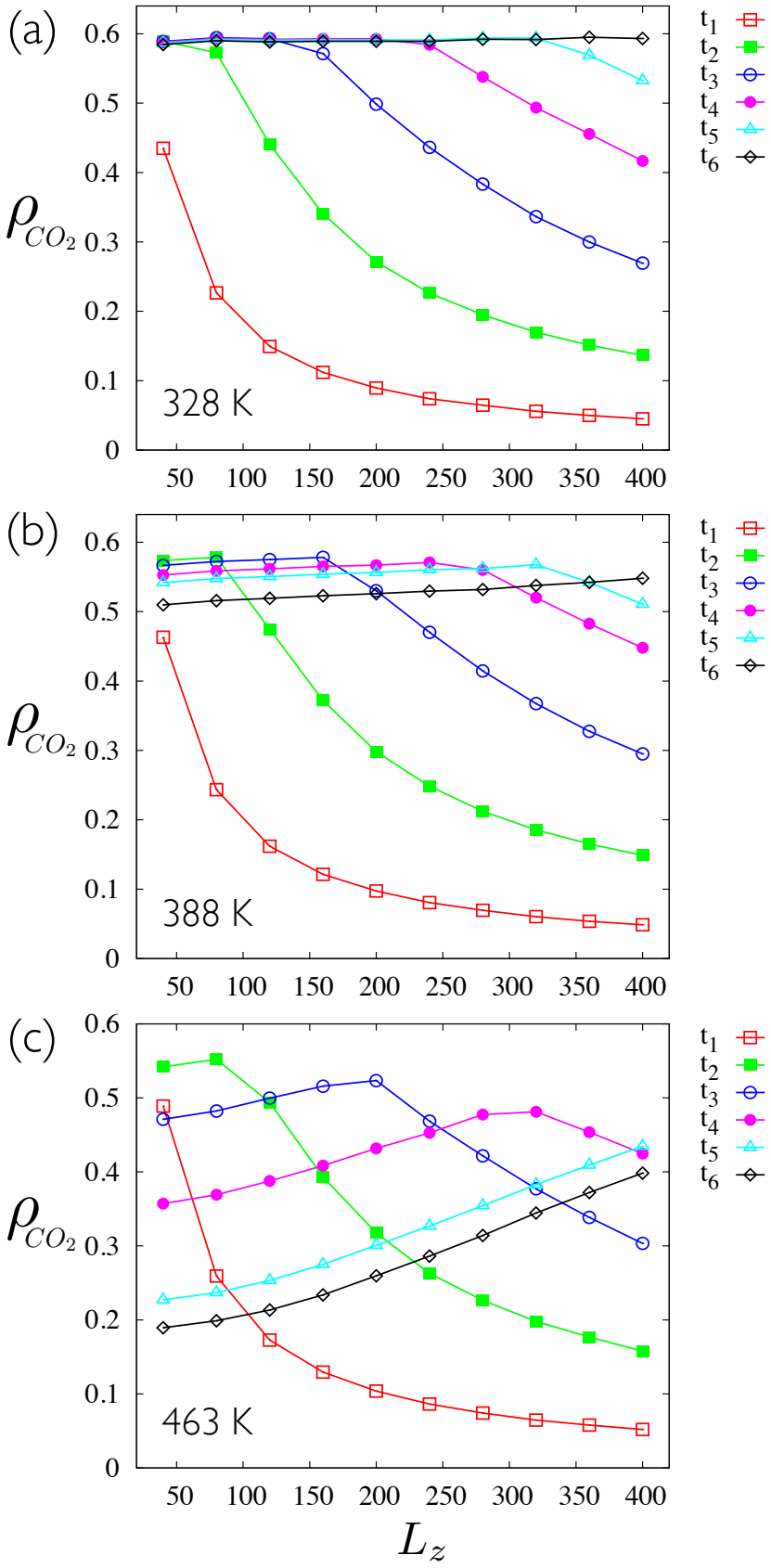

Fig. S5 The total amount of bound CO_2 under nonequilibrium conditions at a given time depends on L_z. We show the fraction of binding sites occupied by CO_2 as a function of L_z at six different times, for $T =$ (a) 328 K, (b) 388 K and (c) 463 K. Here $t_1 < t_2 < t_3 < t_4 < t_5 < t_6$. The data, averaged over 200 independent runs, are for $L_y = 40$. At any temperature T, t_1 and t_6 represent times before and after ρ_{CO_2} reaches its maximum respectively for any L_z. For all the three temperatures, $t_1 \approx 10^4$ (in units of Δt). $t_6 \approx 3.5 \times 10^6$, 3.0×10^6 and 2.4×10^4 (in units of Δt) when $T = 328$ K, 388 K and 463 K respectively.